Modelling of Turbulent SF_6 Switching Arcs

Zhang Q.[1], Yan J. D.[1], Yan G.[2]

[1]*Department of Electrical Engineering and Electronics, the University of Liverpool, Brownlow Hill, Liverpool, L69 3GJ, UK , yaneee@liverpool.ac.uk*
[2]*Henan Pinggao Group Co., Ltd. Nanhuandong Road, Pingdingshan City, 467001, China*

The present work aims at a comparative study of the performance of relevant turbulence models in predicting the behaviour of SF_6 switching arcs during the current zero period. Turbulence models studied include the Prandtl mixing length model, the standard k-ε model and its two variants, i.e. the Chen-Kim model and the RNG model. In order to demonstrate the effects of turbulence, a laminar flow case is also modelled. Based on the computational results, a detailed analysis of the physical mechanisms encompassed in each flow model is given to show the adequacy of each model in describing the rapidly varying arcing process during the current zero period. The computed values of the critical rate of rise of recovery voltage (RRRV) are subject to verification by experimental results covering a wide range of discharge conditions. The relative merits of the flow models are discussed.

Keywords: SF_6 switching arcs, turbulence models, current zero period

1 INTRODUCTION

There is overwhelming experimental and theoretical evidences indicating that an SF_6 arc burning in a converging-diverging nozzle (known as the switching arc) is turbulent and its state close to local thermodynamic equilibrium (LTE) [1]. Such an arcing arrangement is commonly used for the arc interrupter of high voltage circuit breakers (HVCBs). In order to reduce the development cost of HVCBs, it is highly desirable to computationally predict and study the arc behaviour under operational conditions similar to those encountered in a power system. One of the major tasks in achieving full computer aided design of HVCBs is the satisfactory prediction of their thermal interruption capability under turbulent conditions. There is, however, no versatile turbulence model for this purpose with its applicability rigorously verified under different arcing conditions and with different breaker designs. The present work aims at a comparative study of the performance of existing turbulence models in predicting the behaviour of SF_6 switching arcs during the current zero period of an interruption process for which trustable RRRV measurement is available.

Based on the LTE assumption, arc flows in turbulent state are usually described by the time averaged Navier-Stokes equations [2] modified to take into account Ohmic heating and radiation loss in the energy conservation equation. The Boussinesq assumption is used to close the above mentioned conservation equations by relating the Reynolds stress to the gradients of the mean velocity through the concept of eddy viscosity [2]. A turbulence model is therefore required to calculate the eddy viscosity. There are numerous turbulence models reported in the literature [2, 3, 4] but none of them are devised specifically for electric arcs. Modelling of turbulent arcs is still in its infancy, and the mechanisms responsible for the generation of arc instability and the development of arc turbulence are still poorly understood.

There is a direct resemblance between a switching arc and a round free jet, both of which are dominated by shear flow. The most apparent approach for turbulent arc modelling is to start with the examination of the applicability of existing turbulence models, which are devised for shear flows. Of these turbulence models, the Prandtl mixing length model has achieved considerable success in predicting the behaviour of SF_6 switching arcs, notwithstanding the finding that the only turbulence parameter needs to be adjusted, based on test results, for different nozzle geometries [5]. There have been sporadic investigations on turbulent SF_6 arcs using the standard k-ε model [6, 7] and a few of its variants (e.g. using the RNG model [8]), with contradictory claims on the applicability of these models. This is partially caused by a lack of direct verification using reliable measurement of arc

parameters (such as arc voltage, temperature and RRRV) over a sufficiently wide experimental or test conditions.

The present work constitutes a part of our effort towards a versatile turbulence model for switching arcs. The arcing behaviour in a simple two-pressure system is modelled using five flow models, and the test results of Frind et al. [9], Benneson et al. [10] and Frind and Rich [11] are used to judge the relative merits of the models.

2 THE GOVERNING EQUATIONS AND TURBULENCE MODELS

The turbulent switching arc and its surrounding flow are described by the time averaged Navier-Stokes equations modified to take into account Ohmic heating and radiation loss. The arc model has been well reported in [12]. At the electric current level used in the present work, it is sufficiently accurate to calculate the electric field using a simplified Ohm's law [12].

The standard k-ε model [2] and its two variants (the Chen-Kim model [3] and the RNG model [4]) have been chosen for the modelling of turbulent SF_6 switching arcs. Since the application of the Prandtl mixing length model has had considerable success, this turbulence model is included in our investigation for comparison. All these turbulence models belong to the category using the concept of effective eddy viscosity, μ_t. The Reynolds stresses are linearly linked to the main strain via eddy viscosity by means of Boussinesq assumption [2]. The turbulent Prandtl number (Pr_t) provides the link between μ_t (for the momentum equations) and turbulent thermal conductivity, k_t (for the energy equation), which is assumed to be 1 in the present investigation.

In order to demonstrate the effects of turbulence, a laminar case is also included, which is obtained by simply setting μ_t and k_t to zero. For simplicity, the arc models based on laminar flow and turbulent flow will be collectively referred to as the flow models for future reference. Therefore, altogether five flow models are used to study the behaviour of SF_6 switching arcs. The details of the four turbulence models are given below.

2.1 PRANDTL MIXING LENGTH MODEL

This is the simplest and also the oldest turbulence model according to which the eddy viscosity is defined as

$$\mu_t = \rho \ell_m^2 \left(\left| \partial w/\partial r \right| + \left| \partial v/\partial z \right| \right) \tag{1}$$

where the length scale is related to the arc's thermal radius through a turbulence parameter, c, which is given by

$$\ell_m = c \sqrt{\int_0^\infty \left(1 - T_\infty/T\right) \cdot 2r dr} \tag{2}$$

where T_∞ is the temperature near the nozzle wall where the radial temperature gradient is small.

2.2 STANDARD K-EPSILON MODEL

This model is the most widely used turbulence model for engineering applications. The equations of this model are those for the turbulence kinetic energy per unit mass, k, and its dissipation rate, ε, which are given below:

$$\frac{\partial(\rho k)}{\partial t} + \nabla \cdot \left(\rho \vec{V} k - \frac{\rho \nu_t}{\sigma_k} \nabla k \right) = \rho \left(P_k - \varepsilon \right) \tag{3}$$

$$\frac{\partial(\rho \varepsilon)}{\partial t} + \nabla \cdot \left(\rho \vec{V} \varepsilon - \frac{\rho \nu_t}{\sigma_\varepsilon} \nabla \varepsilon \right) = \rho \frac{\varepsilon}{k} \left(C_{1e} P_k - C_{2e} \varepsilon \right) \tag{4}$$

where P_k represents the generation of turbulence kinetic energy due to the mean velocity gradients, which is given by

$$P_k = \nu_t \left[2\left(\frac{\partial w}{\partial z}\right)^2 + 2\left(\frac{\partial v}{\partial r}\right)^2 + 2\left(\frac{v}{r}\right)^2 + \left(\frac{\partial w}{\partial r} + \frac{\partial v}{\partial z}\right)^2 \right] \tag{5}$$

and the eddy viscosity is given by

$$\mu_t = \rho C_\mu k^2/\varepsilon \tag{6}$$

The recommended values of the model constants are [2]: $\sigma_k = 1.0$, $\sigma_\varepsilon = 1.3$, $C_{1e} = 1.44$, $C_{2e} = 1.92$ and $C_\mu = 0.09$.

2.3 CHEN-KIM K-EPSILON MODEL

It has been recognized that the poor prediction of the spread rate of a turbulent round jet by the standard k-ε model is due to the inadequacy of the equation for dissipation rate [3]. For the standard k-ε model a single time scale, k/ε, is used which is an over simplification of the multiple time scales associated with energy transfer between eddies of different sizes [3].

A second time scale related to the production of turbulence kinetic energy is thus introduced to reflect the energy transfer rate from large eddies to small eddies, which is controlled by the production range time scale (k/P_k) and the dissipation rate time scale (k/ε) [3]. The additional source term

$$S_\varepsilon = \frac{\rho C_{3e} P_k^2}{k} \qquad (7)$$

is thus added to the right hand side of equation (4), which allows the dissipation rate equation to respond to the mean strain rate more efficiently, especially in the region where the main strain rate changes rapidly. The recommended values for the model constants are [3]: $\sigma_k = 0.75$, $\sigma_\varepsilon = 1.15$, $C_{1e} = 1.15$, $C_{2e} = 1.90$, $C_{3e} = 0.25$, and $C_\mu = 0.09$.

2.4 RNG K-EPSILON MODEL

The RNG k-ε model is derived from the instantaneous Navier–Stokes equation using a mathematical approach called the renormalization group [4]. The effects of the small eddies are represented by means of a random forcing function in the Navier–Stokes equation. The RNG procedure systematically removes the small scale eddies from the governing equations by expressing their effects in terms of large scale eddies through the modified viscosity (i.e. ν_t in equations (3) and (4) is replaced by the effective viscosity $\nu_{eff} = \nu_l + \nu_t$ where ν_l is the molecular viscosity). In addition, equation (4) contains a strain-dependent correction term which is given by

$$S_\varepsilon = -\frac{\rho C_\mu \eta^3 (1 - \eta/\eta_0)}{1 + \beta\eta^3} \frac{\varepsilon^2}{k} \qquad (8)$$

where $\eta = (k/\varepsilon)\cdot\sqrt{(\rho P_k/\mu_t)}$, $\eta_0 = 4.38$ and $\beta = 0.012$. The other model constants are [4]: $\sigma_k = \sigma_\varepsilon = 0.7194$, $C_{1e} = 1.42$, $C_{2e} = 1.68$ and $C_\mu = 0.0845$.

3 RESULTS AND DISCUSSION

Computations have been carried out for the experimental conditions of Frind et al. [9], Benneson et al. [10] and Frind and Rich [11]. Altogether 3 nozzles with different shapes and dimensions as well as electrode configurations have been studied, which are shown in Fig.1.

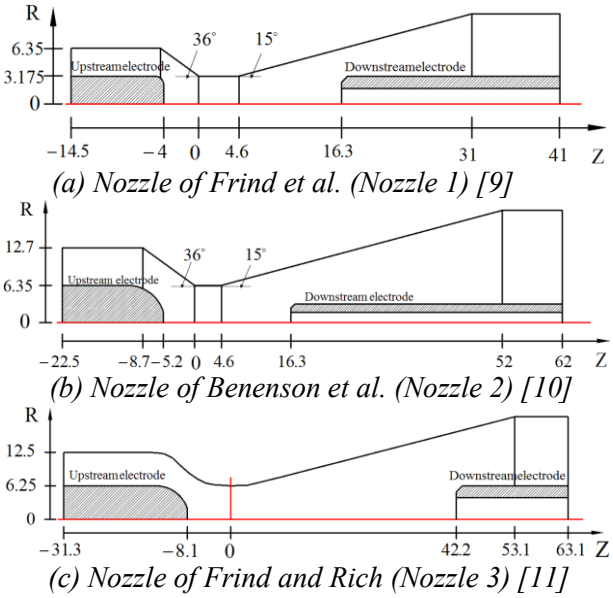

(a) Nozzle of Frind et al. (Nozzle 1) [9]

(b) Nozzle of Benenson et al. (Nozzle 2) [10]

(c) Nozzle of Frind and Rich (Nozzle 3) [11]

Fig.1: Three nozzle configurations used in the GE experiments. Unit of dimensions: mm

Version 3.6.1 of PHOENICS [13] has been used to solve the governing equations. The boundary conditions for the arc conservation equations and the k-ε model equations are detailed in [12]. The flow conditions at the inlet and outlet of the nozzles in Fig.1 are set according to the test conditions reported in [9, 10, 11]. At the nozzle inlet, stagnation pressures (P_0) ranging from 7.8 atm to 37.5 atm are used. At the nozzle exit, a sufficiently low static pressure (P_e) is set for Nozzles 1 and 2, to ensure shock free for the supersonic flow inside the nozzle. For Nozzle 3, $P_e = P_0/4$.

The arcing current is linearly ramped down to zero with a fixed rate of decay, di/dt, from a plateau of 1 kA DC. Two values of di/dt are used for each nozzle, i.e. 13 and 25 $A\mu s^{-1}$ for Nozzles 1 and 2, and, 13.5 and 27 $A\mu s^{-1}$ for Nozzle 3.

For the Prandtl mixing length model, the turbulence parameter, *c*, was adjusted to give the closest agreement between the computed and measured RRRV for a given nozzle geometry. The values of *c* for the three nozzles are respectively 0.054 for Nozzle 1, 0.057 for Nozzle 2 and 0.045 for Nozzle 3.

The qualitative features of computational results for different nozzle configurations, and different values of P_0 and di/dt are similar. Unless otherwise specified, results obtained by the five flow models are given for Nozzle 2 at P_0=21.4 atm and di/dt=13 $A\mu s^{-1}$. Based on

these results, an analysis of the physical mechanisms encompassed in each flow model is given to show the adequacy of a particular model in describing the rapidly varying arc during current zero period.

3.1 ARC BEHAVIOUR BEFORE CURRENT ZERO

The variations of axis temperature and arc radius (defined as the 4000 K isotherm) with axial position at different current levels on the ramp before current zero are, respectively, given in Figs.2 and 3 for those predicted by the standard k-ε model and the Chen-Kim model. Results obtained by the Prandtl mixing length model, the RNG model and the laminar flow model are not given, since the qualitative features of results obtained by the Prandtl mixing length model are the same as those for the standard k-ε model, and results for the RNG model and the laminar flow model are similar to those for the Chen-Kim model.

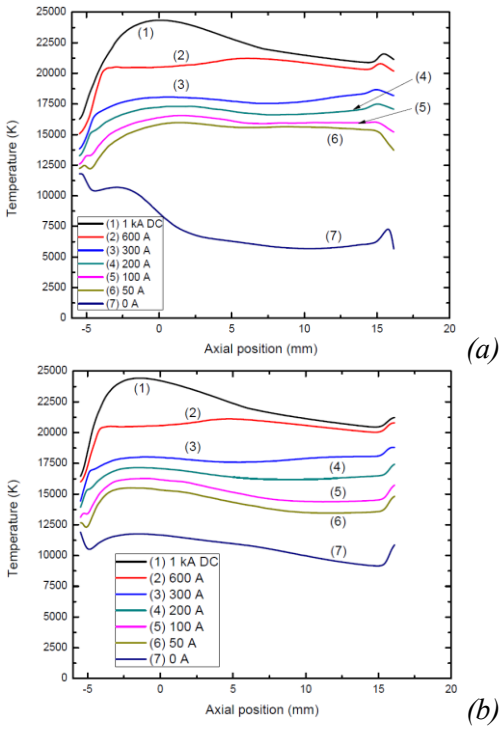

Fig.2: Variation of axis temperature with current decay computed by two flow models.(a) Standard k-ε model and (b) Chen-Kim model

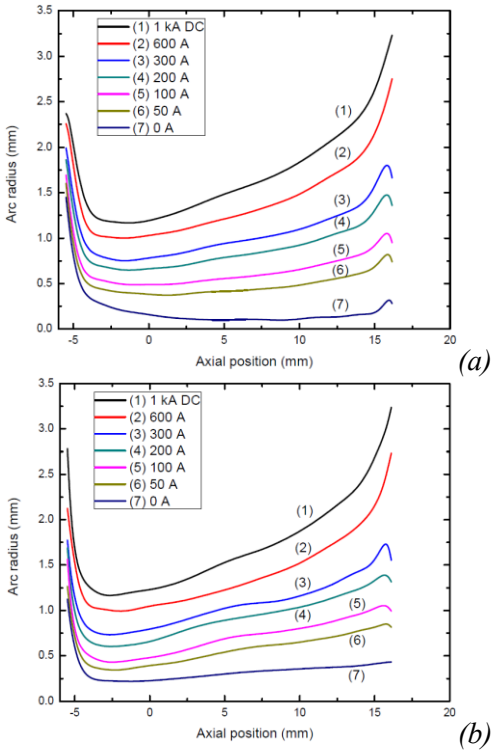

Fig.3: Variation of arc radius with current decay computed by two flow models. (a) Standard k-ε model and (b) Chen-Kim model

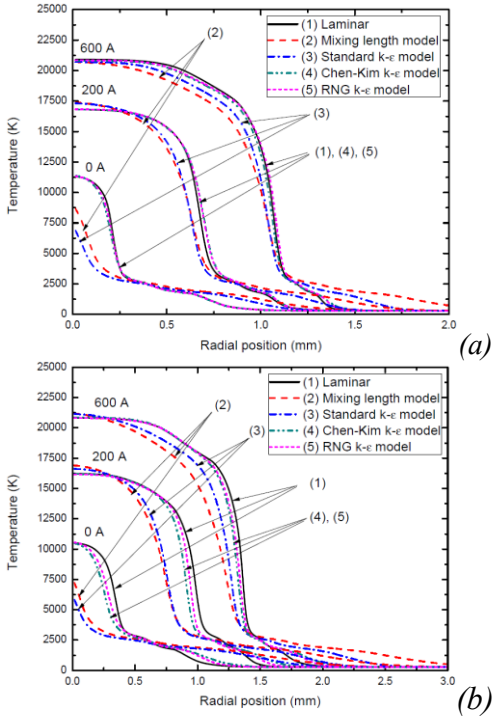

Fig.4: Radial temperature profiles at two axial positions computed by five flow models at three currents before current zero (600 A, 200 A and current zero). (a) Z=2.3 mm and (b) Z=7.9 mm

When the current is large (600 A and above), the axis temperature (Fig.2) and arc radius (Fig.3) predicted by the different flow models show little difference. The axial electric field not only depends on the axis temperature and arc radius but also on the radial temperature profile. Typical radial temperature profiles predicted by the five flow models (e.g. profiles for 600 A in Fig.4) all show a significant high temperature arc core (with the core boundary defined by 83% of the axis temperature), the radius of which is more than 70% of the arc radius for a given axial position, e.g. for Z=7.9 mm and at 600 A, the arc core boundary (predicted by all the five flow models) is around 1 mm and the arc radius is around 1.35 mm (Fig.4(b)). Within this arc core, the temperature is uniform and is not sensitive to flow models. Such temperature profile indicates that within the arc core radiation transport is dominant. Examination of the energy balance reveals that, for all the flow models, radiation is the most important energy transport mechanism inside the arc core.

In the thin layer surrounding the arc core (commonly known as the thermal layer, defined as the region between the arc core boundary and the electrical boundary where the temperature is 4000 K), the energy transport processes predicted by different flow models show significant difference. For laminar flow, Chen-Kim and RNG models, Ohmic heating is balanced collectively by radiation, axial and radial convections, while thermal conduction has the least influence. For the Prandtl mixing length model and the standard k-ε model, turbulent thermal conduction and axial convection are the most important energy loss processes. Thus, the radial temperature profile within this thermal layer (profiles for 600 A in Fig.4) is sensitive to flow models. It is also noted that the turbulence effect predicted by the Prandtl mixing length model is stronger than that of the standard k-ε model, which gives slightly lower temperature (Fig.4). Nevertheless, the thermal layer is very thin in comparison with the high temperature arc core. Therefore, it is found that 80% of the current is conducted within the arc core where radiation is dominant, and thus turbulence has little influence on the arc voltage: the spread in arc voltages computed by the five flow models for the current of 600 A and above is less than 15% of the mean voltage of those predicted by the five flow models (Fig.5). In addition, for all the flow models, the axis temperature is not sensitive to the current (Fig.2), and the arc radius is roughly proportional to the square root of current (Fig.3).The arc voltage is, thus, almost independent of the current (Fig.5) down to approximately 600 A.

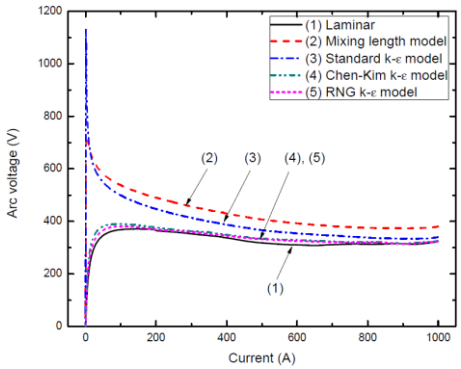

Fig.5: The voltage-current (V-I) characteristics for the nozzle arcs computed by five flow models in the current ramp

It is also found that, for all the flow models applied, up to the core boundary, the rate of change of energy storage accounts for less than 7% of the Ohmic heating for the current of 600 A and above. Since the high temperature core is mainly responsible for conducting the current, the arc at high current can be considered in quasi-steady state, although up to the electrical boundary the rate of energy storage accounts for more than 10% of the Ohmic heating.

When the current is further ramped down towards current zero (below 600 A), the axis temperature is reduced due to weakened Ohmic heating (Fig.2). The dependence of the arc radius on current is found to be stronger than that for currents above 600 A (Fig.3). The arc voltage, therefore, starts to rise with decreasing current (Fig.5). The energy balance based on all the flow models indicate that, from the instant of 200 A, the rate of change of energy storage cannot be neglected in comparison with Ohmic heating and the other energy transport mechanisms, which means the arc deviates from quasi-steady state. We therefore

consider that, from the instant of 200 A, the arc starts to be in its current zero period. During this period, the aerodynamic and electrical behaviour of the arc is significantly affected by the current decay, and the state of arc at current zero is determined by the accumulated effects of arcing heating and cooling from the start of the current zero period to current zero. It should however be noted that the definition of the current zero period is not precise. In high voltage gas blast circuit breakers, the threshold value is around 15 kA for a nozzle radius of 12 – 16 mm [14]. The instant from which the arc transits into the current zero period varies for different discharge conditions, especially the rate of change of current.

During the current zero period, the overall features of the transient arc predicted by different flow models become quite different. It has been found that the axis temperature and arc radius predicted by the standard k-ε model and the Prandtl mixing length model decrease rapidly in the last 4 μs before the current zero (i.e. when the current level is below 50 A, as shown in Figs.2(a) and 3(a)). This is responsible for the formation of an extinction voltage peak shortly before current zero (Fig.5). For laminar flow, Chen-Kim and RNG models, the axis temperature and arc radius show a monotonic decrease when the current is ramped down towards zero (Fig.2(b) and 3(b)), and the rates of decrease of the axis temperature and arc radius are much lower than those predicted by the Prandtl mixing length model and the standard k-ε model. This gives a much longer characteristic time for the variation of arc conductance ($\tau_G = G/|dG/dt|$, where G is the arc conductance) shortly before current zero predicted by these three models, e.g. immediately before current zero, for the Chen-kim model τ_G=0.6 μs, which is much longer than that computed by the standard k-ε model, τ_G=0.04 μs. As a result, the arc voltages predicted by the Chen-Kim, the RNG and the laminar flow models show no extinction peak before current zero (Fig.5).

The large difference in the overall features of the transient arc predicted by different flow models (Figs.2 and 3) during the current zero period, and the resulting difference in the V-I characteristics (Fig.5), indicate that the energy transport processes predicted by these models are very different. Examination of the energy balance reveals that, for the Prandtl mixing length model and the standard k-ε model, turbulence thermal conduction gradually becomes important within both the arc core and at the electrical boundary when the current is further reduced towards zero. Thus, the radial temperature profiles (e.g. profiles for 200 A in Fig.4) computed by these two models have considerable radial temperature gradient inside the arc core. Such strong turbulence cooling is responsible to the rapidly reducing arc temperature shortly before current zero as shown in Figs 2(a) and 4.

For the other three models, inside the arc core radiation loss is still the dominant energy loss mechanism, for which the corresponding radial temperature profile still show an apparent arc core (profiles for 200 A in Fig.4). Up to the electrical boundary, axial convection and radiation loss are important, while turbulent thermal conduction (for Chen-Kim and RNG models only) has the least importance.

At current zero, the very low axis temperature renders radiation loss negligible, and the arc behaviour is determined by energy balance up to the electrical boundary. For laminar flow, the Chen-Kim and RNG models, turbulent thermal conduction (for Chen-Kim and RNG models only), radial and axial convective cooling collectively control the thermal state of the arc. For the Prandtl mixing length model and the standard k-ε model, turbulent thermal conduction and radial convective cooling associated with radial mass inflow are dominant cooling mechanisms. As previously mentioned, during the current ramp, the turbulence effect predicted by the Prandtl mixing length model is stronger than that of the standard k-ε model, and thus the arc voltage predicted by the Prandtl mixing length model is always higher (Fig.5). However, such trend is reserved shortly before current zero, during which the temperature and arc radius reduce very rapidly resulting in lower temperature and smaller arc radius at current zero for the standard k-ε model. This corresponds to the highest voltage extinction peak predicted by

the standard k-ε model (Fig.5), and subsequently over-estimations of the thermal interruption of the nozzle by this model (to be discussed below).

3.2 ARC BEHAVIOUR AFTER CURRENT ZERO

A linearly increasing voltage at a given rate of rise (dV/dt) is used after current zero to investigate the thermal interruption capability of the nozzle configuration. The value of the rate of rise of recovery voltage (dV/dt), at which the arc will just be extinguished, is commonly known as the critical rate of rise of recovery voltage (RRRV). RRRV indicates the thermal interruption capability of the nozzle. This will be found computationally using the five flow models for comparison with the test results.

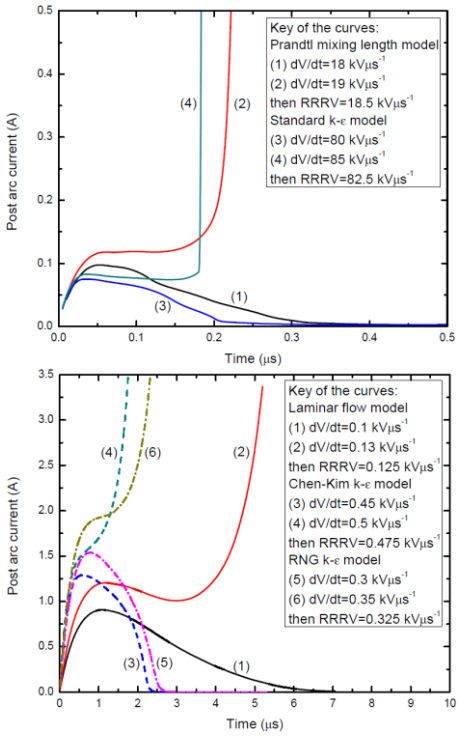

Fig.6: Post-arc current computed by the five flow model

Typical results of post-arc current computed by the five flow models are given in Fig.6. Typical axis temperature and electrical field distributions at different instants after current zero are given in Figs.7 and 8 for the Prandtl mixing length model and the laminar flow model, respectively. Results predicted by the other turbulence models are not given as they are qualitatively similar to those computed by the Prandtl mixing length model.

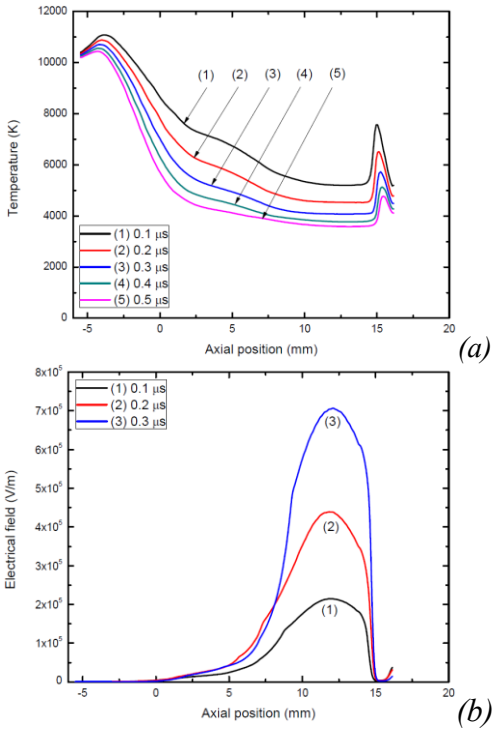

Fig.7: (a) Axis temperature and (b) electrical field distribution at various instants after current zero obtained by the Prandtl mixing length model for $dV/dt=18\ kV\mu s^{-1}$

For the Prandtl mixing length model, when the arc is thermally extinguished, the arc temperature decays rapidly in 0.5 μs after current zero (Fig.7(a)), corresponding to rapid increase of electrical field (Fig.7(b)), in the region of approximately 9 mm downstream of the exit of the flat nozzle throat (i.e. from Z=5 to 14 mm). It is this critical section of the arc that takes up most of the recovery voltage where turbulent thermal conduction and radial inflow cooling are mainly responsible for the rapid cooling of the arc. The standard k-ε model predicts similar arc behaviour after current zero. However, this model predicts a longer critical section than that given by the Prandtl mixing length model, and a more rapid temperature decay rate. This is due to stronger turbulence cooling effects predicted by this model from the instants shortly before current zero as previously discussed. The RRRV computed by the standard k-ε model is therefore significantly higher than that of the Prandtl mixing length model as shown in Fig.6.

The Chen-Kim and RNG models both predict a shorter critical section of the arc and a much slower cooling rate than those predicted by the

Prandtl mixing length model and the standard k-ε model. This is due to much weaker turbulence effects predicted by these two models. The RRRV computed by Chen-Kim and RNG models are therefore of two orders of magnitude lower than that predicted by the other two turbulence models as indicated in Fig.6.

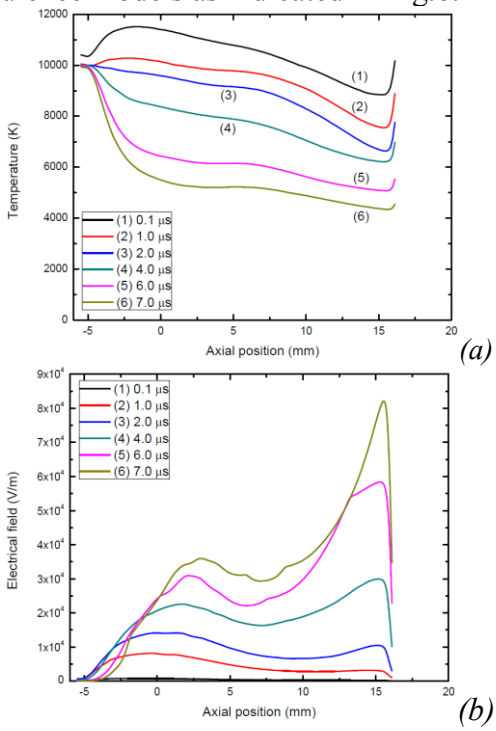

Fig.8: (a) Axis temperature and (b) electrical field distributions at various instants after current zero obtained by the laminar flow model for dV/dt=0.1 $kV\mu s^{-1}$

The laminar flow model predicts a decaying temperature in the whole arc column during the thermal recovery (Fig.8(a)) but the rate of temperature decay is the slowest in comparison with those predicted by the four turbulence models. The electrical field (Fig.8(b)) increases with time due to temperature decay and as a result of axial and radial convective cooling. The peak of the electrical field moves from upstream region to downstream region of the nozzle throat (Fig.8(b)), corresponding to a more rapid rate of temperature decay downstream of the nozzle throat (Fig.8(a)), where axial convection is mainly responsible for arc cooling. RRRV predicted by this model is thus the lowest (Fig.6(b)).

4 COMPARISON WITH EXPERIMENTS

The computed values of RRRV are plotted in Fig.9 together with experimental results given in [10] for comparison. Such a comparison shows that the RRRV predicted by the laminar flow model is a few orders of magnitude lower than that measured, which indicates that turbulence plays a decisive role in the determination of the thermal interruption capability of the nozzle. Of the four turbulence models, the Prandtl mixing length model can generally give satisfactory predictions of the RRRV with optimised turbulence parameter. This is based on the understanding that the turbulence parameter is fixed for each nozzle. The standard k-ε model grossly over-estimates the RRRV for all discharge conditions investigated. The Chen-Kim and RNG models both predict RRRV of the same order of magnitude of that predicted by the laminar flow model. This means these two models significantly underestimate the turbulence effects, and thus they are not capable of predicting the thermal interruption capability of the nozzle.

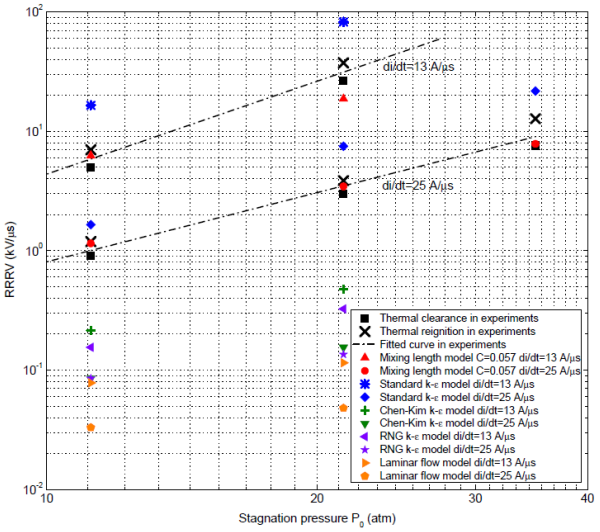

Fig.9: For Nozzle 2: comparison between measured RRRV [10] and predicted RRRV obtained by the five flow models (this work)

It is, however, not sufficient to draw conclusions with regard to the relative merits of turbulence models by comparison of the predicted and measured RRRV based on only one nozzle. We have therefore extended our investigation by considering other nozzle geometries (i.e. Nozzles 1 and 3). Because of the large discrepancy between experimentally measured RRRV and those obtained by laminar flow model and the two variants of the

standard k-ε model, we only test the Prandtl mixing length model and the standard k-ε model. Although the standard k-ε model has grossly over-estimated the RRRV for Nozzle 2, such a conclusion cannot be extended to different nozzles, as it does give good prediction for certain nozzle configuration and discharge conditions (e.g. for Nozzle 1 at P_0=21.4 atm and di/dt=13 Aμs^{-1}) [15]. Comparisons between the predicted and measured RRRV are shown in Fig.10 for Nozzle 1 and Fig.11 for Nozzle 3. Such comparisons show that the standard k-ε model under-estimates the RRRV for Nozzle 1 under most discharge conditions, although it does give satisfactory predictions under certain discharge conditions (e.g. P_0=18 and 21.4 atm and di/dt=13 Aμs^{-1}, Fig.10). Similar to Nozzle 2, the standard k-ε model grossly over-predicts the RRRV in Nozzle 3.

The computed RRRV based on the Prandtl mixing length model agrees well with the measured RRRV for Nozzle 3. For Nozzle 1, it gives reasonable predictions for most discharge conditions except for di/dt=13 Aμs^{-1}. Actually, for all three nozzles, this model gives similar dependence of RRRV on P_0 for different values of di/dt, while the experimental results for Nozzle 1 indicate much stronger pressure dependence at lower di/dt. In theory, the dependence of RRRV on P_0 should not be sensitive to di/dt. If the dependence of RRRV on stagnation pressure is related to di/dt, this will result in the intersection of lines in Fig.10. Such an intersection would imply that at certain range of P_0, the RRRV for a lower di/dt would be smaller than that for a higher di/dt. This is not physical. The experimental results for Nozzle 1 at di/dt=13 μs^{-1} are therefore not very reliable. It is well known that the value of RRRV has a large shot to shot variation. Error bars of the experimental results of [9, 10, 11] are not given. Taking into account the experimental uncertainties, we argue that the predicted RRRV by the Prandtl mixing length model at di/dt=13 Aμs^{-1} for Nozzle 1 is acceptable.

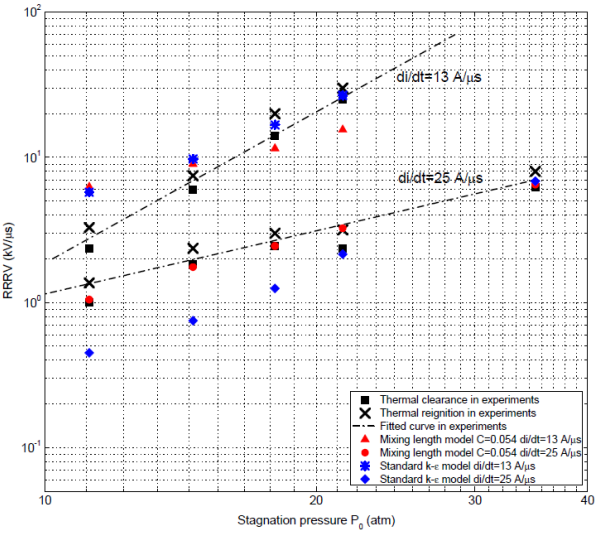

Fig.10: For Nozzle 1: comparison between measured RRRV [9] and predicted RRRV obtained by two flow models (this work)

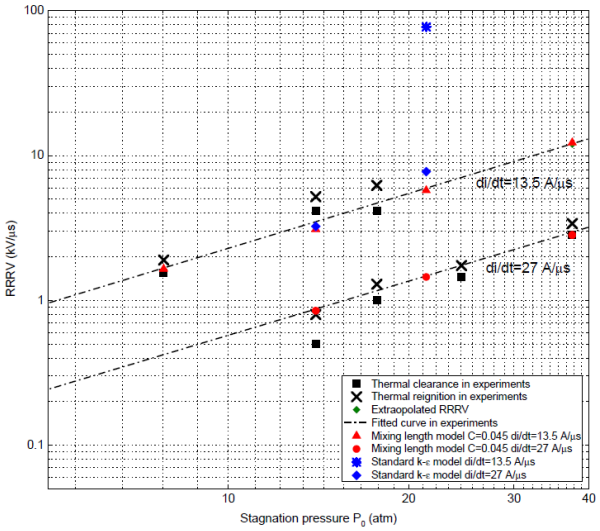

Fig.11: For Nozzle 3: comparison between measured RRRV [11] and predicted RRRV obtained by two flow models (this work)

5 RELATIVE MERITS OF TURBULENCE MODELS

Of the four turbulence models, the standard k-ε model and its two variants, with recommended values of turbulence parameters, cannot give satisfactory predictions on the thermal interruption capability of nozzle arcs under the range of discharge conditions studied, unless further optimizations are made on either turbulence parameters or model equations.

The Prandtl mixing length model can generally give reasonable predictions of RRRV for the range of discharge conditions investigated, although the only turbulence parameter needs to be tuned based on one measured RRRV value. This model is therefore preferred if a known RRRV is available. It is also much easier to implement and the computational cost is the lowest.

6 CONCLUSIONS

The current zero behaviour of SF_6 swiching arcs has been numerically investigated using five flow models: the laminar flow model, the Prandtl mixing length model, the standard k-ε model, the Chen-Kim and the RNG models. These models are assessed by test results produced by GE experiments covering a wide range of discharge conditions [9, 10, 11], and arcs in three nozzle geometries are studied.

Detailed computational results obtained by the five flow models are given for Nozzle 2 at P_0=21.4 atm and di/dt=13 Aus^{-1}. The V-I characteristics of the transient arc are predicted by the five flow models. On the flat part of the V-I characteristics (corresponding to higher currents), 80% of the current is conducted by the high temperature arc core where radiation is the dominant energy loss mechanism. Turbulence therefore has little influence on the arc behaviour at high currents, meaning the arc voltage at high current is not an effective means to verify turbulence models. It is also found that, at high currents, the arc is in quasi-steady state, which means the arc behaviour is not sensitive to the rate of current decay, but only to the instantaneous current.

When the arc is further ramped down towards its zero point, the arc cannot maintain quasi-steady state. Hence, it is known to be in current zero period, when the arc behaviour depends on the rate of current decay. Within this period, thermal conduction due to turbulence effects becomes more and more important due to reduced arc size. The V-I characteristics thus become sensitive to flow models. The Prandtl mixing length model and the standard k-ε model both predict a high voltage extinction peak shortly before current zero, and high RRRV after current zero, due to strong turbulence effects and strong cooling associated with inward cold gas predicted by these two models. The Chen-Kim and RNG models predict much weaker turbulence effects, and thus the computed arc voltages and RRRV are only slightly higher than those predicted by the laminar flow model. Of the four turbulence models, the Prandtl mixing length model gives the best prediction of RRRV when compared with experimental results.

REFERENCES

[1] Zhang Q, Modelling of Turbulence SF_6 Switching arcs, PhD thesis, the University of Liverpool, Liverpool 2014.

[2] Wilcox D C, Turbulence Modeling for CFD, DCW Industries, La Cañada, CA 2006.

[3] Chen Y S, Kim S W, Computation of turbulent flows using an extended k-ε turbulence closure model, Interim report, NASA, CR-179204, 1987.

[4] Yakhot V, Orszag S A, Thangam S, Gatski T B, Speziale C G, Phys Fluids A 4 (1992) 1510-1520.

[5] Fang M T C, Zhuang Q, Guo X J, J Phys D: Appl Phys 27 (1994) 74-83.

[6] Yan J D, Nuttall K I, Fang M T C, J Phys D: Appl Phys 32 (1999) 1401-1406.

[7] Song K D, Lee B Y, Park K, J Korean Phys Soc 45 (2004) 1537–1543.

[8] Bini R, Basse N T, Seeger M, J Phys D: Appl Phys 44 (2011) 025203.

[9] Frind G, Kinsinger R E, Miller R D, Nagamatsu H T, Noeske H O, Fundamental investigation of arc interruption in gas flows EPRI EL-284 (Project 246-1), 1977.

[10] Benenson D M, Frind G, Kinsinger R E, Nagamatsu H T, Noeske H O, Sheer, Jr R E, Fundamental Investigation of Arc Interruption in Gas Flows EPRI EL-1455 (Project 246-2), 1980.

[11] Frind G, Rich J A, IEEE Trans Power Appar Syst 93 (1974) 1675-1684.

[12] Zhang Q, Yan J D, Fang M T C, J Phys D: Appl Phys 47 (2014) 215201.

[13] PHOENICS is the name of a commercial CFD package supplied by CHAM which is based at Bakery House, 40 High Street, Wimbledon Village, London, SW19 5AU, UK.

[14] Yan J D, Han S M, Zhan Y Y, Zhao H F, Fang M T C, Computer simulation of the arcing process in high voltage puffer circuit breakers with hollow contacts, In: Proceedings of FSO2009, Brno, Czech Republic, 2009.

[15] Zhang Q, Liu J, Yan J D, IEEE Trans Plasma Sci 42 (2014) 2726-2727.